Effect of Slurry Processing on the Properties of Catalytically Active **Copper-Alumina Aerogel Material for Applications in Three-Way Catalysis**

Ann M. Anderson, 1* Bradford A. Bruno, 1 Joana Santos, 1 Chris Avanessian 2, Mary K. Carroll 2

¹Department of Mechanical Engineering and ²Department of Chemistry

Union College, Schenectady, NY 12308 USA

*Corresponding author: andersoa@union.edu, ORCID 0000-0002-4055-2518

ABSTRACT

This study examines the catalytic performance of copper-alumina (CuAI) aerogel which is a

possible alternative to the use of precious metals in automotive exhaust treatment systems which require

simultaneous conversion of carbon monoxide, unburnt hydrocarbons and nitrogen oxides. To be a viable

alternative, the aerogel materials need to withstand a slurrying process to enable coating onto a substrate

and they need to maintain performance in a humid environment typical of what is seen in automotive

exhaust. In this study, we slurried heat-treated copper-alumina aerogels in an acidic (pH ~4) aqueous

solution under mechanical stirring. The solution was subsequently dried at 60 °C under ambient pressure

conditions. Physical properties of slurried CuAl aerogel (surface area, X-ray diffraction, morphology) were

similar to those of non-slurried materials. Catalytic testing in a simulated automotive exhaust

environment demonstrated that the aerogels can survive exposure to humidity. The ability of the slurried

and non-slurried aerogels to oxidize propene and carbon monoxide was similar under dry and humid

conditions. In a high-O₂ environment adding humidity degraded catalytic performance while in a low-O₂

environment the humidity improved performance. The catalytic performance of the nitrogen monoxide

was less consistent: the slurried sample did not perform as well as the non-slurried sample under any

conditions.

KEYWORDS: Aerogel catalyst, Three-way catalyst, Copper-alumina aerogel, Slurry

ACKNOWLEDGEMENTS

This material is based upon work supported by the National Science Foundation (NSF) under Grants No.

IIP-1918217, IIP-1823899, DMR-1828144 and CBET-1228851. The funding source was not involved in

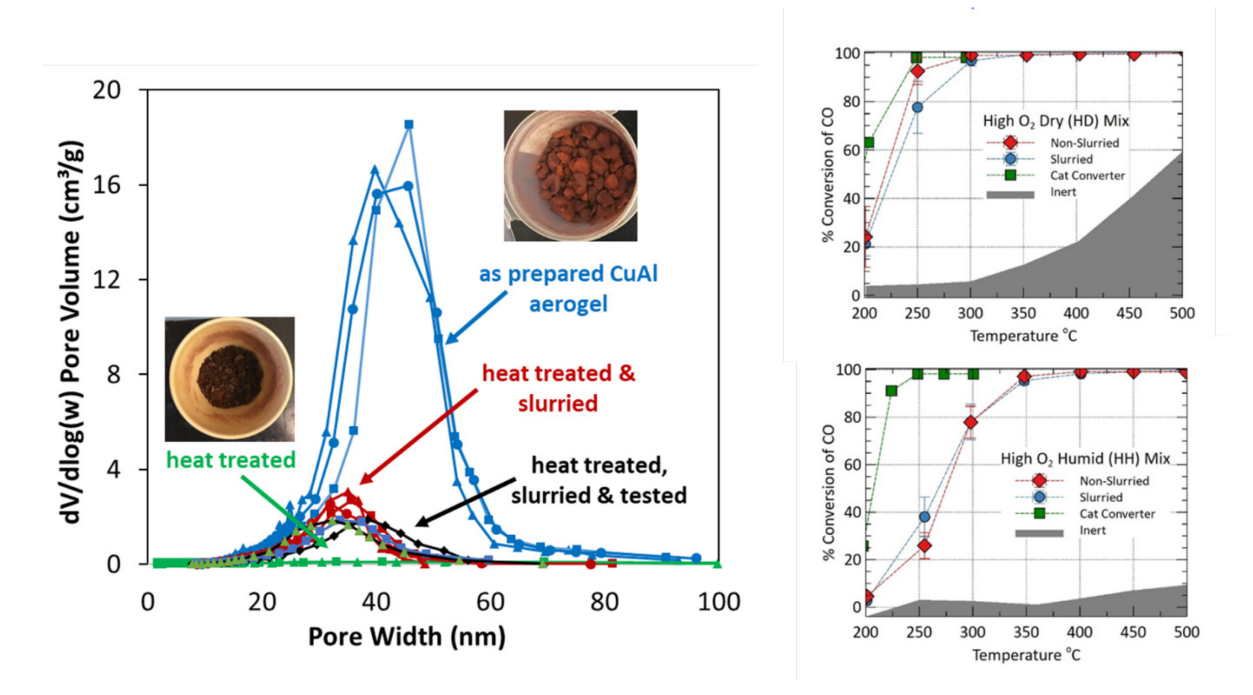
conducting this research or preparing the manuscript. We thank Diana Lang for preliminary experimental

work and Chris O'Brien for help with the UCAT testing. We are grateful to Rebecca Cortez and Yijing Stehle

for discussions regarding interpretation of the AFM data.

1

GRAPHICAL ABSTRACT



Caption: Copper-alumina aerogels can be slurried and exposed to a humid exhaust stream and maintain three-way catalytic performance. The figures on the left show images of the material as prepared, after heat treatment and via atomic force microscopy. Pore volume is reduced after heat treatment and slurrying. The images on the right show catalytic performance for CO in dry and humid conditions.

HIGHLIGHTS

- Slurried copper-alumina aerogel largely maintains its physical structure
- Slurried copper-alumina aerogel shows three-way catalytic activity
- Copper-alumina aerogel is catalytically active in a humid simulated exhaust stream
- Light-off temperatures for copper-alumina aerogel are higher in humid exhaust

1. Introduction

Aerogels have significant potential for development as heterogeneous catalysts. They are easily tailored for catalytic activity by combining one or more catalytically active metal species including non-precious group metals (PGMs) with an aerogel support matrix. The aerogel matrix itself offers high surface area, high porosity, low density and good thermal stability. Due to these properties, a range of types of aerogel have been synthesized for various photocatalytic and catalytic applications [1-4].

Gasoline engines produce exhaust that includes a wide variety of harmful components such as unburned hydrocarbons (HCs), carbon monoxide (CO), various nitrogen oxides (NOx), and relatively small quantities of particulates. Of these HCs, CO, and NOx are historically the primary regulated pollutants. The current industry standard solution used to address these three pollutants in gasoline engines is a "catalytic

converter" or three-way catalyst (TWC). A typical automotive TWC, housed in a metal casing, consists of a cordierite support onto which a PGM-containing alumina washcoat is applied. A washcoat is typically formed by an aqueous, catalyst-containing slurry that is applied to a support to form a porous oxide layer. A TWC is capable of simultaneously reducing the level of HCs, CO and NOx found in gasoline engine exhaust by 90% or more under normal operating conditions [5].

Despite their efficacy, conventional TWCs have some shortcomings. First, the use of PGMs in TWCs is problematic. Not only are PGMs expensive, but the methods used to mine them are environmentally damaging [6]. Second, while quite effective under normal operating conditions, TWCs do not work well until they reach a sufficient temperature (ca. 250 °C) to catalyze the required reactions. For example, 60-80% of the total HCs emitted during testing under the Federal Test Procedure are emitted during the cold start (the initial ca. 2 min) of the test, before the TWC can achieve light off, the point at which 50% conversion of a pollutant has been achieved [7]. Hence alternative materials made from non-PGM catalysts are of interest to the automotive industry.

We are interested in exploiting aerogel properties for use in TWC applications, which specifically require simultaneous conversion of carbon monoxide, unburnt hydrocarbons and nitrogen oxides. This is an area that has not yet been well studied; but we note that catalytic aerogels, including those under study here, are potentially of interest for other applications as well. There are several mechanisms by which aerogels could potentially improve the performance of TWCs. First, the high specific surface area of aerogel material results in more active sites and improved gas/solid interaction, thus promoting catalytic reactions and potentially reducing the metal loadings required to reach a needed level of conversion. Second, because they are made using sol-gel methods it is possible to tailor the chemistry to a specific application [1]. This tailorability could reduce or even eliminate the need for the use of PGMs. Finally, two distinct thermal effects could allow aerogels to reduce the time required for a TWC to light off. The first of these is that aerogel's high temperature stability [8-10] could reduce the susceptibility of active sites in the washcoat to diffusion/sintering. For example, Bouck et al. [9] showed that aluminabased aerogels underwent the expected phase transformation from boehmite to γ-alumina when heated to 500 °C but resisted further changes in samples heated to 1100 °C. This could allow the TWC to be placed in hotter regions, closer to the engine, thereby reducing heat loss and leading to shorter light-off times. The second thermal effect is that aerogels have low thermal inertia, so their use could reduce the time needed to reach light-off temperature regardless of where it is placed relative to the engine.

We have synthesized a number of catalytic aerogels using a rapid supercritical extraction (RSCE) method [11-14]. When tested in dry granular form, using a simulated dry automotive exhaust mixture,

these materials show activity as TWCs [15-18], able to reduce NO and oxidize HCs and CO with light-off temperatures in the 220-425 °C range. Of those studied by our group the copper-alumina (CuAl) aerogels were found to have the best overall performance (showing, for example, CO light-off temperatures as low as 220 °C) and so were selected for further study. While the initial performance of these materials is quite promising, several open questions remain about their use in TWC applications, primarily because of aerogels' reputation for being fragile and the effect that water (in liquid or vapor form) could have on the aerogel nanostructure and its properties. It is important to know whether these materials can survive exposure to a humid exhaust stream typical of what is found in the real automotive application and still provide TWC capability. There is some research on the effect of water vapor on aerogels (for example in insulating materials [19]), however we are not aware of any work on the effect of humidity on aerogels specifically for TWC applications (which require the simultaneous conversion of NO, HC and CO).

It is also important to determine whether these materials can be processed in ways that would allow them to be used in practical application (i.e. can they be cast on to a typical TWC support structure such as cordierite). There are several studies that have investigated approaches to incorporating aerogel in a cordierite structure. Armor and Carlson [20] added open-form supports (including cordierite honeycomb) to silica and chromia aerogel precursor solutions and then performed high-temperature supercritical extraction with the support in situ. They found there was good adhesion between the aerogel and the support and also noted that the aerogel material penetrated into the pores of the open-form structures. Dominguez et al. coated cordierite monoliths with Co-SiO₂ [21] and Co-Fe-Si [22] aerogel for an ethanol steam reforming application by dip-coating the cordierite into a silica sol just before gelation to form a wet gel on the surface. The monolith was subsequently soaked in an ethanol solution of cobalt nitrate and/or iron nitrate for three days and then processed via high-temperature supercritical extraction. SEM images of the resulting aerogel-coated cordierite showed that the material was well deposited on the surface and had penetrated into the cordierite pores. Preliminary experiments indicate that this approach is compatible with the RSCE aerogel fabrication process employed in our laboratory; however, it would likely have a high barrier to entry in the established catalytic converter manufacturing industry.

A more compatible approach would be to integrate aerogel directly into the automotive industry-standard washcoating process. This process involves making a slurry of catalytically active material (typically alumina with a formulation of precious metals) and applying it to the cordierite substrate. Aerogel slurries have been made from the powdered form of silica aerogels and have been used, for example, to impregnate aerogel into fabric to make highly insulating blankets [23]. In a catalysis

application, Landau et al. [24] combined a chromia aerogel powder with a boehmite binder and rotary washcoated the mixture onto the surface of α -Al₂O₃ ceramic foam to prepare a catalyst for combustion of chlorinated volatile organic compounds. They found that this method resulted in a more uniform coating and better control of the chromia loading than did dip-coating methods.

This work extends our previous studies of aerogels as TWC materials to: (1) assess the effects of slurrying to determine if these materials can be incorporated into the standard washcoating process and maintain TWC performance and (2) assess the effects of a humid environment on the ability of these materials to convert all three pollutants. We have synthesized copper-alumina aerogels, slurried them in an aqueous solution and measured physical and catalytic properties. Our methods and results are described in detail below.

2. Experimental

2.1 Materials

The precursor salts aluminum chloride hexahydrate AlCl₃•6H₂O (99%) and copper(II) nitrate trihydrate Cu(NO₃)₂•3H₂O (99%) were purchased from Sigma Aldrich, as was an epoxide, propylene oxide (>99%), used in the gelation process. Fisher Scientific was the source for denatured (reagent-grade) ethanol, absolute ethanol, and concentrated nitric acid. In-house deionized (DI) water was used to prepare the dilute nitric acid solution. All materials were used as received, without additional purification.

2.2 Gel Formation

Copper-alumina (CuAl) wet gels were prepared using an impregnation method described previously [13, 15, 18]. In the first step of the process, an alumina gel was formed through an epoxide-assisted process [10]: dissolving 11.84 g of aluminum chloride hexahydrate into 80 mL of reagent-grade ethanol (~2 h), and then adding 17 mL of the proton scavenger propylene oxide while stirring with a magnetic stir bar until gelation occurred (typically within 15 min). The beaker was then sealed with plastic paraffin film and left to age in a fume hood. After 24 h any excess solvent was poured off and the gel was broken into smaller pieces. The gel was then exposed to a solution of 8 g of copper(II) nitrate trihydrate in 80 mL of absolute ethanol for 24 h, which served both to introduce copper into the matrix and remove excess propylene oxide, other reagents and byproducts via solvent exchange. After 24 h, the liquid was poured off and a fresh aliquot of 80 mL absolute ethanol was poured onto the copper-impregnated wet gels for solvent exchange over a second 24-h period. Following one additional solvent exchange (80 mL absolute ethanol for 24 h), excess solvent was poured off and the wet gels were processed to yield aerogels. Note that approximately 65% of the copper from the salt was incorporated into the gel through

this process, with the remainder poured off in the ethanol used for impregnation and solvent exchanges [18].

2.3 Aerogel Fabrication

A rapid supercritical extraction (RSCE) method developed at Union College [11-13] was used to dry the wet gels. The method uses a metal mold and hot press and the wet gels were processed as described in [18] by placing the wet gels into the wells of a stainless-steel mold and topping off the wells with ethanol. The mold was sandwiched between two gaskets (made from stainless steel foil/graphite) and placed on the bottom platen of a Tetrahedron 24-ton MTP-14 hydraulic hot press. The mold was sealed and heated to 249 °C using a load of 200 kN to ensure that the conditions in the mold exceed ethanol's critical point. The press force was then decreased to allow the supercritical fluid to escape and the mold was cooled to room temperature. The entire RSCE process took approximately 5 h.

2.4 Heat Treatment & Slurrying Process

Loosely covered Pyrex crucibles containing the aerogel pieces were placed in a programmable Thermo-Scientific Thermolyne furnace. All aerogel samples were heat treated (calcined) at 800° C for 20-24 h under ambient conditions prior to catalytic testing. Select heat-treated samples were slurried by adding 10 mL of heat-treated aerogel to 50 mL of an acidic (~pH 4) solution prepared from concentrated nitric acid and deionized (DI) water, in order to approximate the pH of typical commercial washcoating processes. The beaker was covered with paraffin film and placed on a mechanical stirrer and stirred for approximately 1.5 h. The paraffin film was then loosened and the solution was heated to 60 C for 1-4 h with continued stirring, and then allowed to dry fully under ambient conditions in a fume hood.

2.5 Characterization Methods

2.5.1 Bulk Density

Bulk density was determined by measuring the volume of samples of known mass. Due to the nature of the samples (coarse powders) the measurement is crude and tends to overpredict the volume, thus underpredicting the actual bulk density.

2.5.2 Gas Adsorption

A Micromeritics ASAP 2020 Gas Adsorption system was used to measure the surface area, pore volume and pore distribution of the CuAl aerogels in various forms (as prepared, heat treated and slurried). The aerogels were first gently crushed using a mortar and pestle. Then ~0.2 g of aerogel was placed in a sample tube and degassed by heating to 90 °C for 2 h and then 200 °C for 6 h. After degassing, the sample was analyzed using the ASAP 2020 with a 20- to 50-s equilibration time. Longer equilibration

times were used at high partial pressures to avoid the effects of compression at high pressure [25]. BET surface area was determined using five points at relative partial pressures from 0 to 0.3. BJH pore distributions and pore volume were evaluated using the desorption isotherms. Multiple samples in each form were tested.

2.5.3 Powder X-Ray Diffraction

Powder XRD patterns were acquired and analyzed using a Rigaku Powder SE X-ray diffractometer equipped with a copper X-ray source tube and a nickel filter. Each sample was crushed into a powder and packed into a 0.5-mm-deep well of a glass sample holder. Diffraction patterns were taken over a 2θ range of 5°–80° using a tube voltage of 40 keV and a 45-mA current. All samples were analyzed using the Bragg-Brentano mode with a step size of 0.03°, a speed of 15°/min and an incident slit of 1°. The XRD pattern peaks were matched using the Rigaku SmartLab Studio II.

2.5.4 Scanning Electron Microscopy (SEM)

Aerogel powder was pressed onto standard 12.7-mm-diameter SEM pin-stub mount (Ted Pella, Inc) covered in double-sided carbon tape. No conductive coating was used in the analysis. SEM images were obtained with a ZEISS EVO MA-15 SEM in High Vacuum mode. A working distance of ca. 8 mm, accelerating voltage of 15.00 kV, filament current of 2.000 A, and a spot size of 500 (unitless) were used for imaging. Energy dispersive X-ray (EDX) maps were obtained with a Bruker XFlash 6 | 30 detector coupled to the SEM instrument. The detector was held at -28.0 °C. Topographical images were obtained using backscattered electron (BSE) detection, and no image filter was used. Oxygen, aluminum and copper maps were imaged with signal collected for ~3 min for each map.

2.5.5 Atomic Force Microscopy (AFM)

Samples were prepared for imaging by spreading one layer of clear high-gloss nail top coat (essie gel-setter) onto a standard glass microscope slide using the included brush. A spatula was then used to sprinkle small amounts of powdery sample onto the covered portion of the slide. Once the top coat was dry, a gloved finger was dragged across the sample surface in order to break off any aerogel pieces protruding from the dried top coat, and this produced flat aerogel fracture surfaces. AFM images were obtained with an Oxford Instruments Asylum Research MFP-3D AFM in AC (tapping) Air Topography mode using a MikroMasch model HQ:NSC14/Al BS probe mounted on a standard cantilever holder. Images were taken using a scan rate of 1.00 Hz and a resolution of 256 points & lines. The scan angle was always set to zero. The integral gain was set between 2.6 and 10, depending on the image.

2.5.6 Catalytic Testing

The Union Catalytic Aerogel Testbed (UCAT) was used to measure the catalytic ability of the aerogels. It is shown schematically in Figure 1 and described more fully in Bruno et al. [26]. Two separate 23 ± 2 mL CuAl samples were placed in two identical packed-bed test sections, which in turn were placed in a furnace (ThermCraft 9800W Split Tube) controlled by the UCAT system to maintain the samples at the desired temperature set point during a test. The temperature of the gases flowing through the aerogel beds was monitored by thermocouples placed in the inlet and outlet flows of the packed beds.

A separate gas mixing and bottling system (not shown) was used to make a custom blend of pollutants which included a hydrocarbon (propene), nitrogen monoxide (NO), and carbon monoxide (CO). The resulting bottled simulant (labeled "core blend" on the schematic, Figure 1) was then connected to the UCAT system. All test condition mixtures used in this work started from this same "core blend" of bottled gas (described below). Oxygen was not added at the bottling stage (to maintain storability of the core blend) nor was water (to avoid condensation in the bottle); instead, when desired, oxygen and/or water were added by the UCAT flow control and humidification systems. Oxygen addition occurred via air addition (modeled as 1 O_2 : 3.76 N_2) to the test section flow stream prior to heating. Humidity, when used, was added as liquid DI water, metered by syringe pumps and vaporized by preheaters prior to reaching the oven and packed bed test sections. The UCAT flow system metered the flow of gas through the test sections to maintain a constant selected space velocity across the full temperature range of the test, regardless of the quantity of air and/or humidity added to the "core blend" used to simulate various engine exhaust conditions.

For the tests performed in this study we used exhaust simulant blend recipes based on US Drive Recommendations [27] for simulating fuel-rich and fuel-lean gasoline engine exhaust conditions, with some notable modifications. First, to avoid complexities due to the five-gas analyzer's differential response to different hydrocarbons, pure propene was used as the HC component rather than the US Drive suggested blend of HCs. (We note that prior testing of the copper containing CAMs has been performed using a different simulated exhaust blend containing propane [26].) Second, all four test conditions / test mixtures used in this study started with the same core blend and were then mixed with different quantities of O_2 (from air) or water in order to arrive at the desired test condition. Both of these modifications led to slight shifts in the values of the "Stoichiometry Number," S, defined by Schlatter [28] as:

$$S = \frac{2O_2 + NO}{CO + H_2 + 3nC_nH_{2n} + (3n+1)C_nH_{2n+2}}$$

for each of the four test mixtures used. (Each chemical symbol in the calculation of the stoichiometry number represents the volumetric concentration of gas.) Full details of each mix used and the US Drive recommended blends are provided in Table 1. Finally, a constant space velocity of ca. 61,200 h⁻¹ (approximating the higher 60,000 h⁻¹ space velocity recommend by US drive for powdered catalysts and conditions under which "clearer discrimination among the candidate catalysts is desired") [27] was selected for all testing.

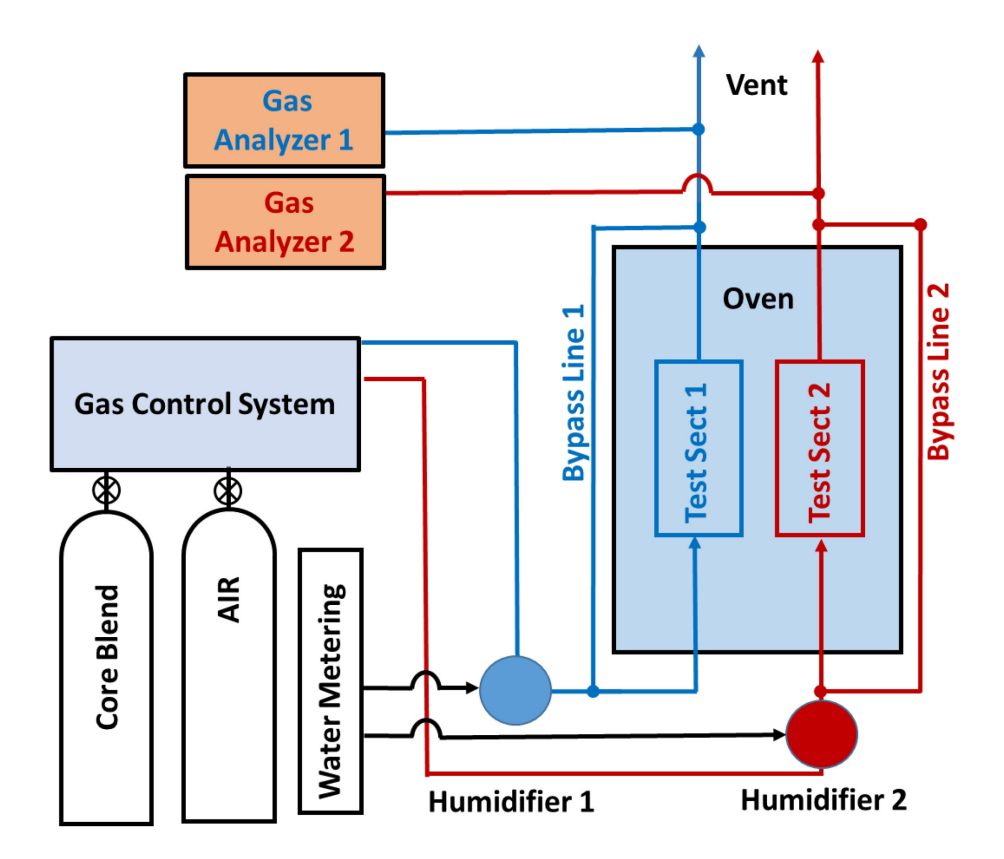


Fig. 1. Schematic of UCAT system. The core blend and air are metered by the gas control system and sent into the two test sections containing the samples to be tested. The temperature is maintained at steady state by the oven. Two five-gas analyzers, one for each test section, alternately measure the input concentrations through the bypass line and the output (i.e. catalyst-treated) concentrations at the oven exit.

Table 1. Volumetric composition of simulated exhaust gas mixtures used in this study. US Drive recommended blend [27] provided for comparison.

	Mixture Component							
Mixture	HC	NO	CO	H ₂	CO ₂	H ₂ O	O ₂	Stoichiometry
US Drive [27], Recommended	(ppm) Ethene:525 Propene:500 Propane:150	(ppm) 1000	0.5	0.17	13	13	(%) 0.12-1.15	Number 0.2145-1.514
Modified Case HD High O ₂ /Dry	Propene: 1125	1125	0.56	0.19	14.6	0	1.15	1.36
Modified Case LD Low O ₂ /Dry	Propene: 1183	1183	0.59	0.20	15.4	0	0.12	0.193
Modified Case HH High O ₂ /Humid	Propene: 970	970	0.49	0.17	12.63	13	1.15	1.57
Modified Case LH Low O ₂ /Humid	Propene: 1028	1028	0.52	1754	13.39	13	0.12	0.212

Pollutant concentrations were measured at steady-state temperatures ranging from 200 to 500 °C at approximately 50 °C intervals using a commercial five-gas analyzer (Infrared Industries FGA4000XDS 5 Gas Analyzer, one per test cell). At each test condition, concentrations of the three pollutants (CO, NO, and HC) as well as CO2, and O2 were measured. The known, untreated, gas concentrations were measured (via the bypass lines) prior to the first two temperature conditions for each gas condition and again during the last temperature condition, to monitor for any instrument drift during each set of testing. The conversion efficiency was then calculated from these measurements. The temperature reported is the average of the inlet and outlet gas flow temperatures for each test section. The difference between the inlet and outlet temperature was maintained at typically <5 °C, maximally <10 °C. For each type of aerogel (slurried or non-slurried) we ran two separate samples (one in each test section) through three to five full temperature sweeps under each of the four conditions defined in Table 1 (HD, LD, HH, LH). Although these tests do not perfectly mimic actual automotive-use conditions or US Drive protocols, perhaps most notably with regard to the high-frequency transient oxidizing/reducing flow dithering present with modern automotive-emissions-control schemes, they do bracket a broad swath of the required performance range for catalysts within TWCs and so provide a useful tool for screening the likely TWC potential of various catalytic aerogel materials.

3. Results & Discussion

3.1 Aerogel Appearance

Photographs of as-prepared copper-alumina (CuAl) aerogel are shown in Figure 2a. After heat treatment, the volume is reduced by a factor of about four as shown in Figure 2b. Slurrying further reduces the volume by about 50% (not shown). The heat-treated and slurried aerogels are denser (see Table 2) and more robust than the as-prepared materials.

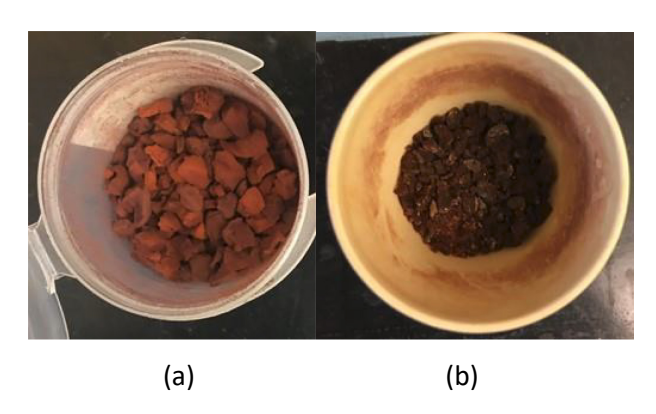


Fig. 2. Photographs of CuAl aerogel (a) as prepared, and (b) post heat treatment.

3.2 Bulk Density, Surface Area & Pore Distribution

Bulk density, BET surface area and pore volume results are presented in Table 2 for as-prepared, heat treated non-slurried (HT), and heat-treated and slurried (SL) samples. The bulk density presented for the as-prepared, heat treated non-slurried (HT) samples is the average of 37 samples ± 1 standard deviation. The bulk density presented for the heat treated and slurried (SL) is the average of 16 samples ± 1 standard deviation. The surface area and pore volume presented are averages of three to four measurements (except for the catalytically-tested material, which is from a single run). The uncertainty in surface area is based on the BET fit and the mass measurement uncertainty. The uncertainty in pore volume is based on the mass measurement uncertainty.

The as-prepared materials have low bulk density (0.12 g/mL), high surface area (336 m²/g) and high pore volume (3.5 cm³/g). After heat treatment, the pore volume and surface area decrease, likely due to pore collapse via sintering, and the bulk density increases. After slurrying, the bulk density further increases; there is no significant change to surface area but the pore volume increases slightly. After catalytic testing with humid air the surface area and pore volume remain similar to their values pretesting, indicating that the water vapor in the simulated exhaust gas does not alter the structure of the aerogel.

Table 2. Effect of heat treatment and slurrying on physical properties of CuAl aerogel materials.

Treatment	Bulk Density (g/mL)	Surface Area (m²/g)	Pore Volume (cm³/g)
As-Prepared	0.12 ± 0.02	336 ± 17	3.5 ± 0.2
Heat-Treated	0.30 ± 0.04	65 ± 3	0.12 ± 0.01
& dry catalytically tested		64 ± 3	0.13 ± 0.01
& humid catalytically tested		61 ± 4	0.14 ± 0.01
Heat-Treated & Slurried	0.6 ± 0.1	67 ± 3	0.54 ± 0.02
& dry catalytically tested		70 ± 3	0.52 ± 0.02
& humid catalytically tested		59 ± 3	0.47 ± 0.02

Figure 3a compares the adsorption/desorption isotherms for the CuAl aerogel samples in different forms. Figure 3b plots the corresponding desorption-based BJH pore distributions. The as-prepared materials show a broad peak in the 20-60 nm range, centered around 40-43 nm. These pores are no longer present after heat treatment, with the pore distribution showing low pore volume (0.12 cm³/g) and no identifiable peaks. Surprisingly, after slurrying, the pore volume increases to about 0.5 cm³/g and the distribution shows a small peak in the 20-50 nm range. This increase after exposure to the aqueous solution was unexpected and is an area of ongoing investigation.

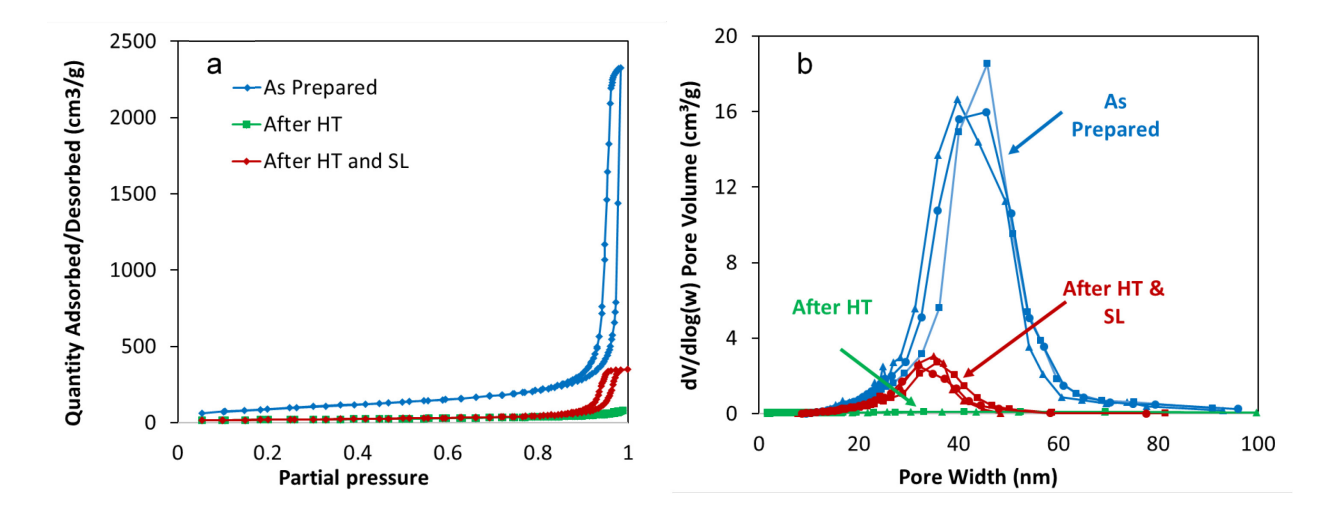


Fig. 3. Gas adsorption results for various forms of CuAl aerogels: as prepared (in blue), after heat treatment (HT, in green) and after heat treatment and slurrying (HT+SL, in red): (left) Adsorption/desorption isotherms and (right) BJH desorption-based pore distributions for two or three distinct samples. Lines are provided as a guide to the eye.

3.3 Powder X-Ray Diffraction

Powder XRD results are plotted in Figure 4 for the as-prepared, heat-treated, heat-treated/slurried and dry catalytically tested aerogels. The XRD pattern of the as-prepared sample is consistent with previous work [9, 10,15]: peaks at $2\theta = 28^{\circ}$, 49° and 65° indicate the presence of the pseudoboehmite form of alumina. The additional peaks are attributed to a copper-containing crystalline species [15, 29]. The patterns for the heat-treated and heat-treated/slurried materials are identical, with peaks at $2\theta = 31^{\circ}$, 37° , 45° , 58° , 60° and 66° attributable to a copper aluminate spinel (CuAl₂O₄, ICDD PDF-2 Card 01-075-4272). 'Sidewings' observed around the peak at 37° and the peak at 50° for the catalytically -tested sample are consistent with previous work [15] and match to copper(II) oxide (CuO, ICDD PDF-2 card 01-080-1917).

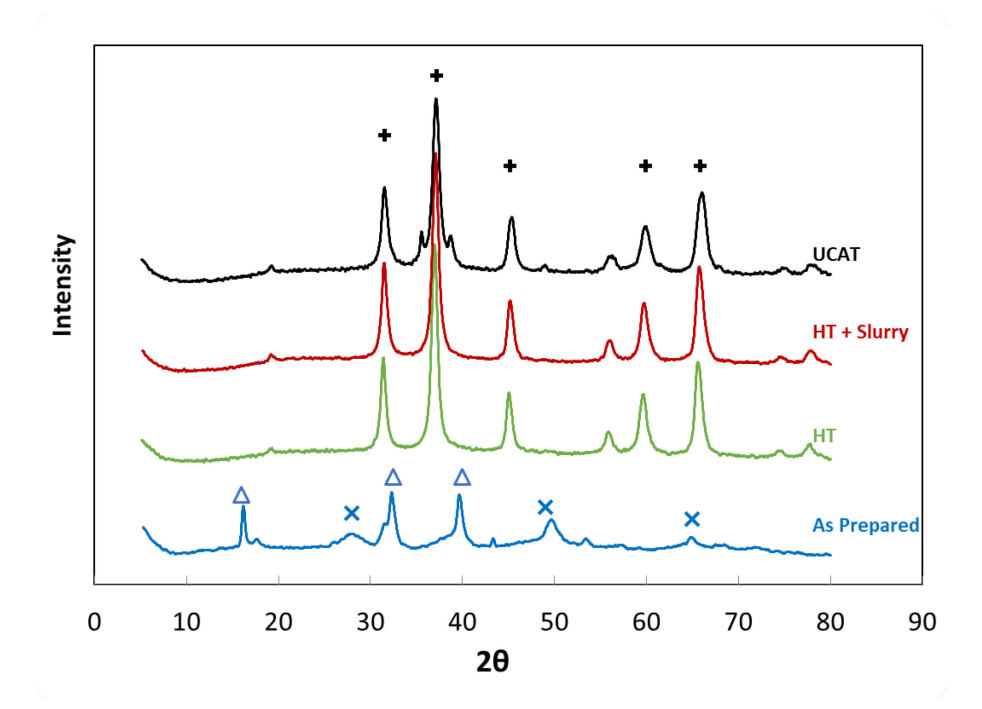


Fig. 4. XRD patterns for as prepared, heat treated (HT), slurried (HT + Slurry) and dry catalytically-tested CuAl aerogel materials (UCAT). Patterns are offset for clarity. Black crosses (+) are used to indicate peaks attributed to a CuAl $_2$ O $_4$ spinel; blue crosses (x) indicate peaks attributable to pseudoboehmite; green triangles (Δ) indicate peaks attributable to a copper-containing crystalline species [15, 29].

3.4 SEM/EDX Imaging

Figure 5 shows a compilation of SEM and EDX images of the slurried aerogel after it had been catalytically tested. The SEM image (Fig. 5a) shows the typical aerogel-like morphology seen in other catalytic aerogels. The EDX image and maps (Figs 5b-e) show evidence of copper-containing particles that

are 150-300 nm in diameter. The oxygen map indicates that these are a copper oxide which is consistent with the XRD pattern for UCAT-tested aerogels. These SEM images are similar to those for the non-slurried materials [18].

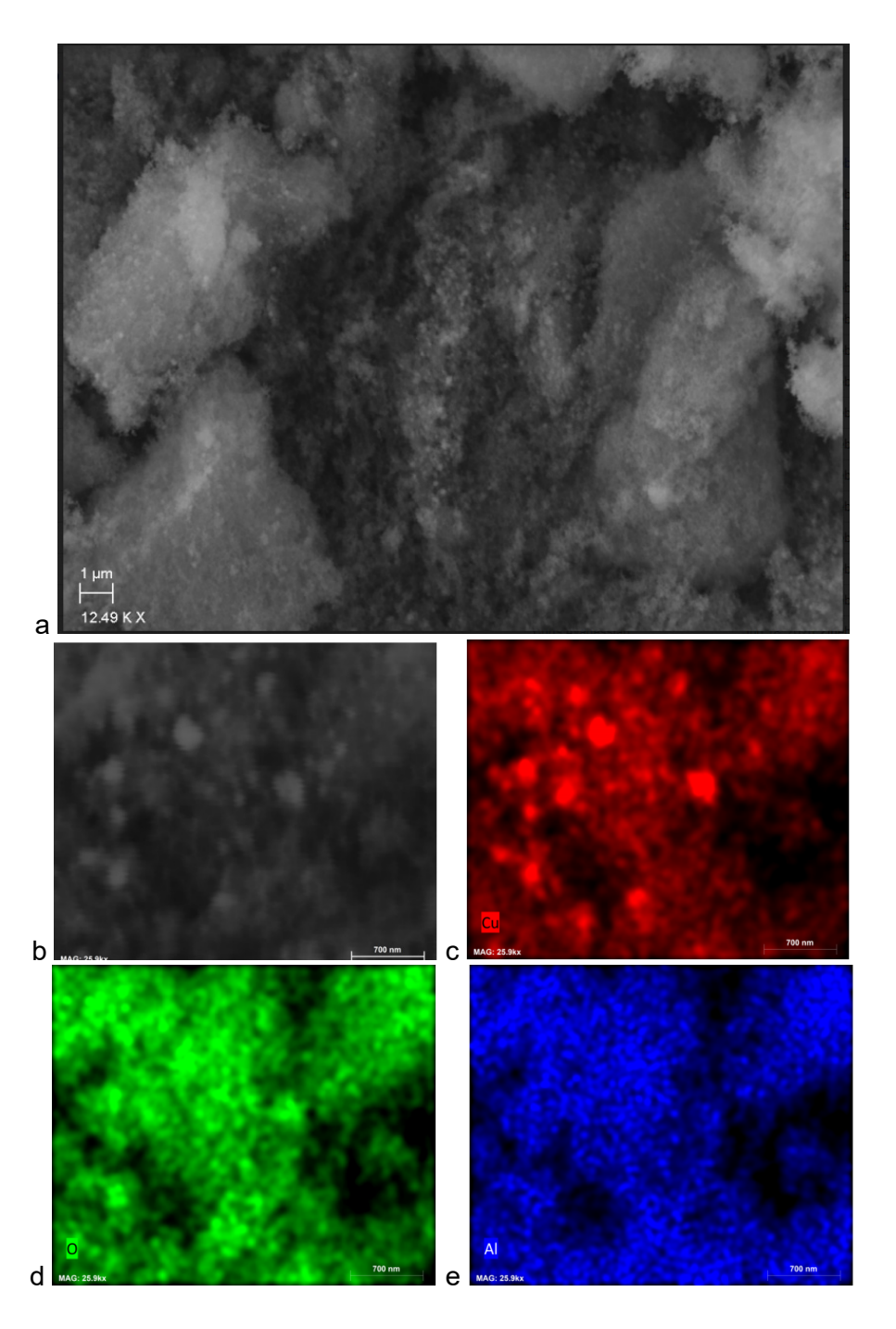


Fig. 5. SEM images of the slurried CuAl aerogel material (a) at 12.5kx magnification (b) at 26K magnification (700-nm scale bar) and corresponding EDX images showing (c) copper, (d) oxygen and (e) aluminum content.

3.5 AFM Imaging

AFM images of as-prepared, heat-treated, and heat-treated/slurried CuAl aerogels are shown in Figure 6. Aerogels are difficult to image by AFM. Here we present the highest-magnification images obtainable for each sample; as a consequence, the scale is not the same in the various views, so care must be taken when comparing the images. Clusters of 30-50 nm in diameter are visible in all images. The image of the as-prepared material (Figure 6a) shows agglomeration of the clusters into larger (200-400 nm) aggregates. In the image of the heat-treated material (Figure 6b), the clusters appear to be more densely packed. This is in agreement with the reduction of surface area, pore volume and increase in bulk density seen for heat-treated versus as-prepared aerogels (Table 2).

Figure 6c shows an AFM image of the heat-treated and slurried CuAl sample, which is similar to the heat-treated (non-slurried) aerogels with perhaps more dark regions indicating increased porosity. This agrees with prior surface area results that showed that the slurrying process does not significantly change the structure of CuAl aerogel but did result in a slightly more porous material. The image of the slurried aerogel (Figure 6c) appears smeared from left to right; however, we believe this is an artifact due to the probe tip dragging across the sample as it scanned in the left-to-right direction.

3.6 Catalytic Performance

Repeated tests were performed on the non-slurried and slurried CuAl aerogel materials under both dry and humid exhaust conditions. (Details of the conditions along with the abbreviations used in this discussion are provided in Table 1.) To provide context and comparison, tests were also performed on inert (silica) aerogel and on a 15-mL sample cored from a conventional, commercially available TWC (NAPA universal converter, part # 15037).

For the dry-gas test conditions (HD and LD) and high-O₂ humid (HH) conditions, results were repeatable with time (i.e. we observed no evidence of aging of the materials). Typical results are presented in Figure 7, which plots CO conversion results for five repeated temperature-sweep runs of the slurried aerogel tested under high-O₂-with-humidity (HH) conditions. Here, two samples of the slurried aerogel were tested simultaneously. While there are minor sample-to-sample differences observed, likely due to slight variations in testing conditions (e.g., sample packing differences, between the two test sections), the results are fairly consistent, with a light-off temperature of 250-275 °C and full conversion by ~350 °C. As expected, there is more scatter in the data around the light-off point, due to uncertainty in the test-section temperature (which typically varied about 5 °C from the inlet to the outlet). The repeatability of the results is typical of what was obtained for the HC, CO and NO performance under high

O₂ conditions (both humid and dry). The samples show no aging effects. In this case, by the fifth run, the materials had been tested for over 30 h with no performance degradation.

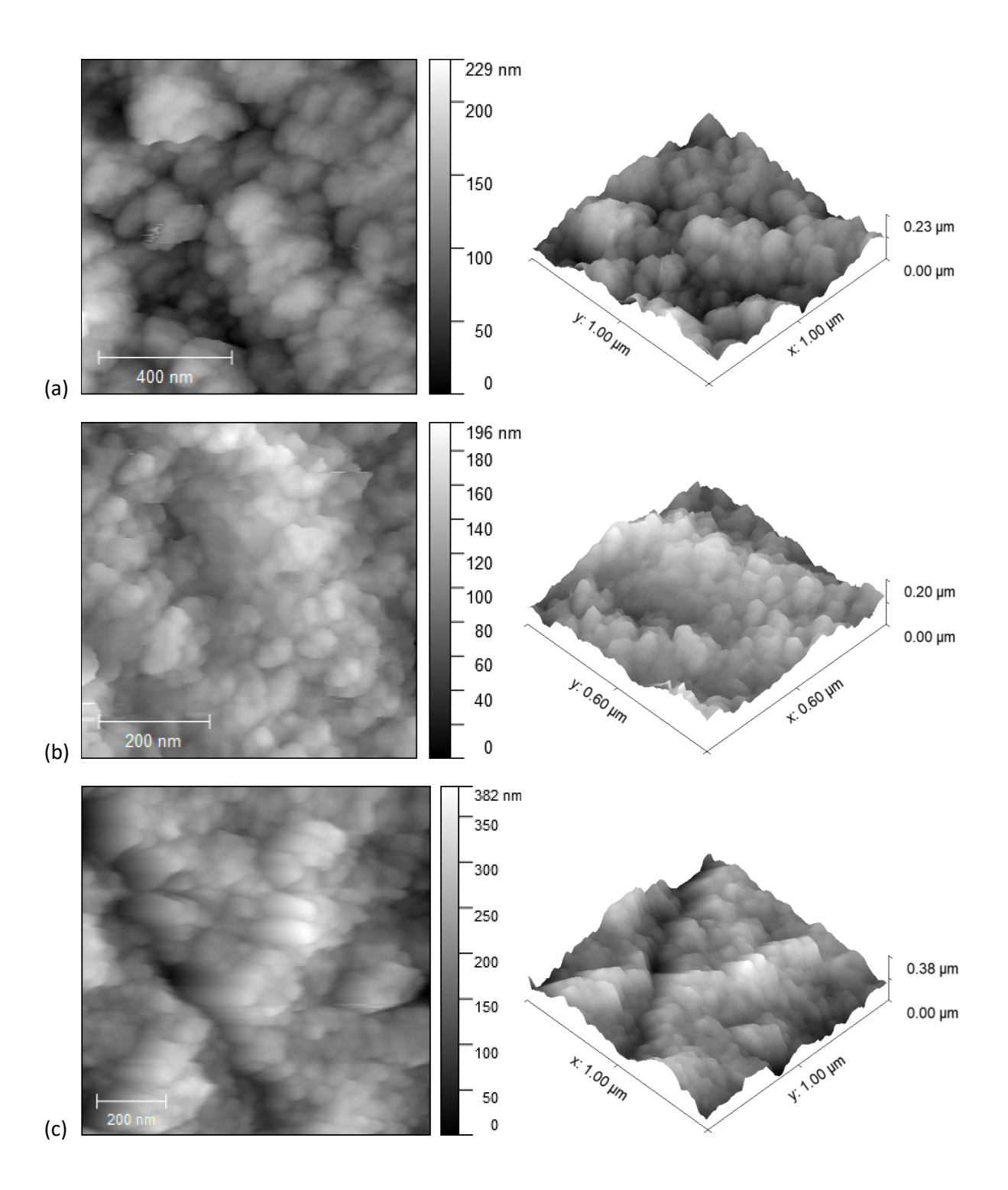


Fig. 6. AFM images of (a) as-prepared CuAl aerogel (b) heat-treated CuAl aerogel and (c) heat-treated and slurried CuAl aerogel. Note: not all images are at the same scale.

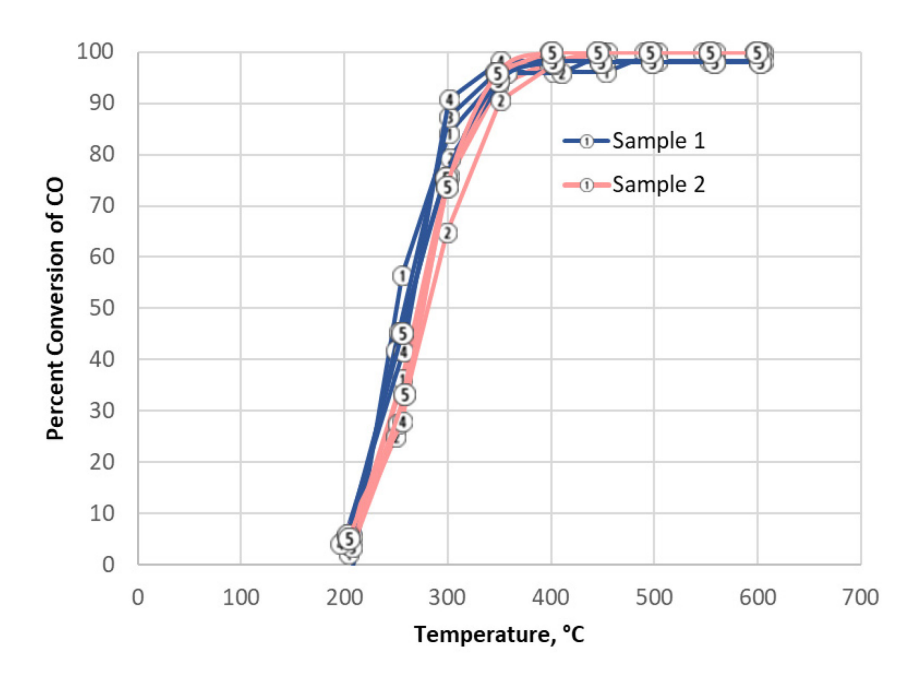


Fig. 7. Percent conversion of CO as a function of temperature for the slurried CuAl aerogel sample under high O_2 humid (HH) conditions. Numbers on data points correspond to data from individual tests. Lines are provided as a guide to the eye.

However, there is evidence of some sort of initial aging or conditioning effect evident in the NO data under low-O₂ humid (LH) conditions. Figure 8 shows the NO conversion results for three repeated temperature-sweep runs of the non-slurried aerogel tested under low-O₂-with-humidity (LH) conditions. Two samples of the non-slurried aerogel were tested simultaneously. It is worth noting when considering these data that, due to instrument sensitivities, the NO data typically show more scatter and are less repeatable than for the other two pollutants, especially at low conversion rates. Regardless, there is clearly a significant difference between run 1 and runs 2 and 3, indicating that some sort of aging or conditioning effect occurs during the sample's first exposure to humid conditions. We saw this behavior in the NO, CO and HC conversions for both slurried and non-slurried samples when samples were first tested under humid conditions. This behavior did not occur under dry conditions. For the LH tests, only runs subsequent to the first were included in averaging.

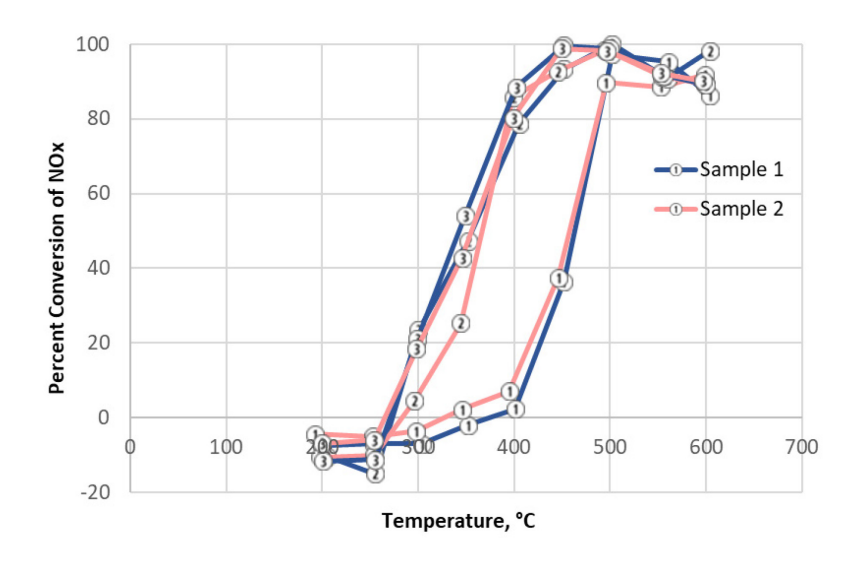


Fig. 8. Percent conversion of NO as a function of temperature for the non-slurried sample under low- O_2 humid (LH) conditions. Numbers on data points correspond to the individual tests. Lines are provided as a guide to the eye.

Figures 9 and 10 show the catalytic performance of both slurried and non-slurried CuAl aerogels under dry and humid conditions respectively. The figures also include conversion data for an in-house-prepared [12] inert silica aerogel (shaded region) and for the sample cored from the commercial catalytic converter (NAPA universal converter, part # 15037). The averages were calculated combining data from both test sections for repeated tests (i.e. temperature sweeps). In both of these figures the most important conditions, from the point of view of TWC performance, are the top two plots in the left-hand column (showing oxidation of HCs and CO under favorable conditions) and the bottom plot of the right column (showing reduction of NO under favorable conditions). In an actual automotive TWC application the engine control system will cause conditions to oscillate between the high-O₂ and low-O₂ conditions at a frequency of about 1 Hz. This oscillation is critical to the performance of the TWC as it allows opportunities for specific conversion reactions to occur under favorable conditions. Typically, materials with oxygen-storage capability (e.g., ceria) and other components are added to the catalyst mix to leverage this effect and further enhance performance.

Figure 9 compares the average percent conversions of HC, CO and NO for the slurried and non-slurried materials under dry catalytic test conditions. For high-O₂ conditions (Figure 9, left column) there is no significant difference in performance between the non-slurried and the slurried aerogels for the two important oxidation reactions, with light off at about 250 °C for HC and 220 °C for CO. Unsurprisingly, this performance is somewhat poorer than for the PGM-containing commercial catalysts, which light off 30-40 °C earlier. The CuAl catalyst shows negligible conversion of NO as is to be expected for this oxidizing

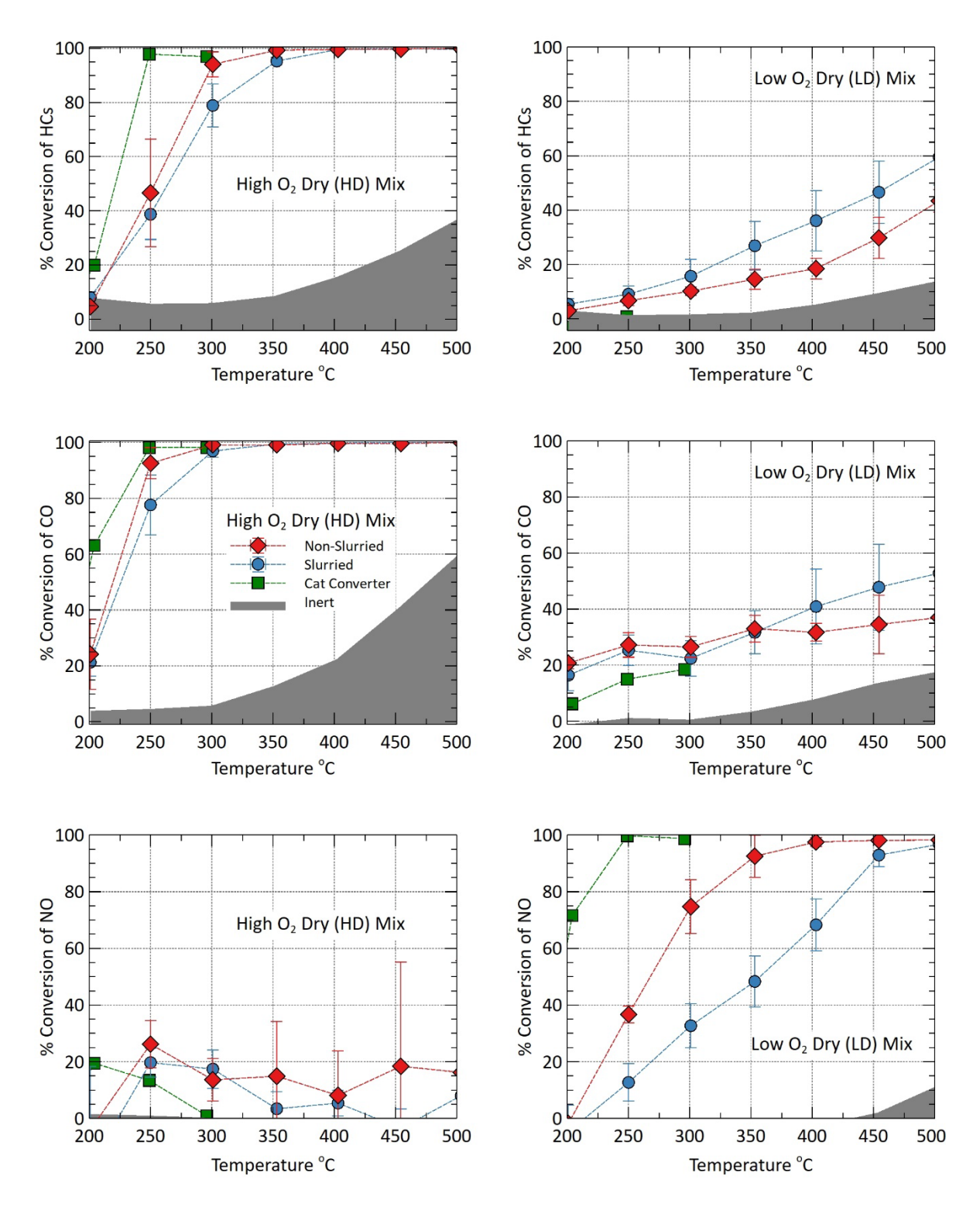


Fig. 9. Catalytic data for non-slurried CuAl aerogel (red diamonds), slurried CuAl aerogel (blue circles), commercial catalyst (green squares) and inert silica aerogel (grey-shaded region) under dry conditions with high O_2 (left column) and low O_2 (right column). Error bars represent \pm 1 standard deviation in 2-4 temperature sweeps. Lines are provided as a guide to the eye.

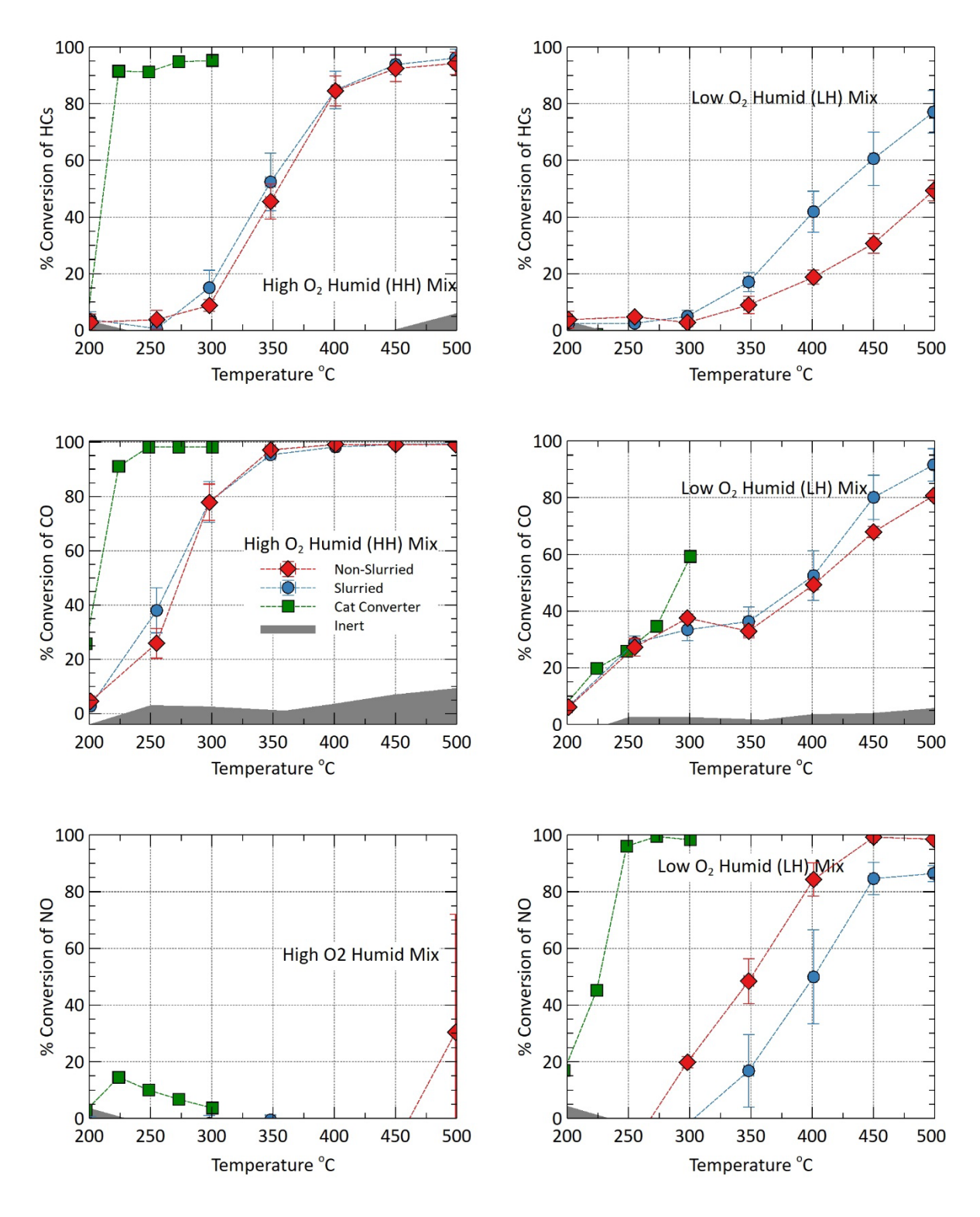


Fig. 10. Catalytic data for non-slurried CuAl aerogel (red diamonds), slurried CuAl aerogel (blue circles), commercial catalyst (green squares), and inert silica aerogel (grey-shaded region) under humid conditions with high O_2 (left column) and low O_2 (right column). Error bars represent \pm 1 standard deviation in 6 temperature sweeps. Lines are provided as a guide to the eye.

(high-S, high-O₂) environment, as does the commercial catalyst. Under low-O₂ conditions (Figure 9, right column) the slurried material performs similarly to the non-slurried for conversion of CO and slightly better than the non-slurried for the conversion of HCs. However, as expected, neither oxidation reaction reaches 50% conversion at commercially interesting (below ca. 300°C) temperatures for either the aerogel or the commercial catalyst under these unfavorable oxidizing conditions. Under these low-O₂, low-S conditions, which favor reduction, the CuAl aerogel catalyst does achieve light off for NO conversion at 260 °C for the non-slurried and 350 °C for the slurried material, both significantly higher than the light-off temperature of the commercial catalyst. To reiterate, under dry conditions and as measured by light-off temperature under favorable conditions, slurrying the aerogel catalyst does not affect its CO or HC oxidation performance measurably, but it does degrade its NO reduction performance somewhat.

Figure 10 compares the average percent conversions of HC, CO and NO for the slurried and non-slurried material under humid catalytic test conditions. Again, for high-O₂ conditions (Figure 10, left column) there is no significant difference in performance between the non-slurried and the slurried aerogels. Under low-O₂ conditions (Figure 10, right column) the slurried material performs slightly better than the non-slurried for the conversion of HCs, comparably to the non-slurried for the conversion of CO and worse for the conversion of NO, as it did under dry catalytic test conditions.

The most significant difference in performance between the slurried and non-slurried samples occurs for the NO reduction reactions under favorable (low O₂) conditions. These data show a decrease in performance for the slurried materials. There is evidence, albeit weaker, for a slight increase in performance for the oxidation of hydrocarbons under globally reducing (low O₂) conditions. Although potentially interesting, this improvement would not be considered important to the usefulness of these materials in TWCs (HC oxidation under reducing conditions is not a key performance metric). No other cases show evidence for significant differences in performance (positive or negative) between the slurried and non-slurried materials. The most notable physical difference between the slurried and non-slurried materials is in their pore volume, which could be expected to affect conversion. However, since the performance of one set of reactions (HC oxidation under globally reducing conditions) is increased while another is decreased (NO reduction under globally reducing conditions) and all others are unchanged, this simple explanation is likely insufficient. The question as to the causes of the (relatively few) performance differences between the slurried and non-slurried materials is an important topic for future work.

Comparing Figures 9 and 10 allows us to examine the effect of humidity on the performance of these aerogel-based catalysts. First, under oxidizing (high-S) conditions there is a clear decrease in the performance of both the slurried and non-slurried materials under humid versus dry conditions. The light-

off temperature for HC oxidation increases by approximately 100 °C between the HD and HH test conditions, and the light-off temperature of CO oxidation increases by about 50 °C. The already minimal conversion of NO is further suppressed upon the shift from HD to HH conditions. When making these humid/dry comparisons it is important to recall that the way the test gases are mixed in our experiments results in slight shifts in S value (stoichiometry number) between the humid and dry test gases (see Table 1). Thus, it is important to differentiate differences in performance caused by humidity from differences caused by changes in S. In all cases the addition of humidity makes our test blends slightly more oxidizing. For the high- O_2 cases just considered the S value shifts from S = 1.36 for the HD case to S = 1.57 for the HH case. So, based only on the favorability of the test gas for oxidizing, one would have expected slightly improved performance under the humid conditions and so the observed decrease in performance must be a real effect of the inclusion of water in the gas. Goncalves et al. [30] reported a similar, but not as severe, decrease in performance of a copper nanoparticle catalyst for CO oxidation under humid conditions and attributed the effect to "the adsorption of water on the catalyst surface." We note that the degradation in performance just described is reversible. Samples tested in a dry environment after they had been tested in a humid environment returned to the dry performance level, and this perhaps provides further evidence of some sort of water adsorption mechanism being at play.

Under low-O₂ (low-S) conditions the conversion of HC and CO are somewhat improved, especially at higher temperatures, in the humid condition (although the conversions are still rather low overall). This effect is likely explained by the presence of H₂O enabling CO destruction via the water gas shift reaction and destruction of HCs via the steam reforming reaction; both reactions that play well-known roles in TWC applications [31]. NO conversion under low-O₂ conditions is also suppressed with the addition of humidity, with light-off temperatures increasing by approximately 90 °C for the better-performing non-slurried catalyst, 50 °C for the slurried catalyst and 35 °C for the commercial catalyst. Light-off temperatures for an inert sample (silica), the non-slurried aerogel, the slurried aerogel and a sample of commercial catalytic converter material are summarized in Table 3.

Table 3. Light-off temperatures* for aerogels tested under dry and humid conditions.

	HC		С	0	NO	
Catalyst	High O₂	Low O ₂	High O ₂	Low O ₂	High O₂	Low O ₂
Silica	/	/	475/	/	/	/
CuAl Non- Slurried	250/350	/500	220/270	/400	/	260/350
CuAl Slurried	260/350	460/425	220/270	500/400	/	350/400
Commercial	220/210	/	190/210	/290	/	190/225

^{*} Values given in °C for dry (left)/humid (right) conditions

4. CONCLUSION

We have demonstrated that a copper-alumina aerogel can be slurried without significant degradation of physical and catalytic properties. Moreover, we have demonstrated that an alumina-aerogel-based catalyst can survive and perform (i.e. oxidize HCs and CO, and reduce NO) in a humid exhaust stream, as would be experienced in a gasoline exhaust pollution mitigation (TWC) application. Comparisons with an existing commercial PGM-based catalyst indicate that the light-off performance demonstrated by the relatively simple CuAl aerogel catalyst formulations (single active species) tested herein is insufficient to allow them to replace the use of PGMs in TWCs. However, this is not surprising since modern TWC catalysts typically include mixtures of several active components (most commonly platinum, palladium, rhodium and ceria), each tailored to enhance the overall performance of the TWC. Finally, the focus of the present work is on demonstrating the robustness of the catalytic aerogel materials, rather than elucidating the mechanisms by which they perform TWC. Although SEM/EDX and powder XRD analyses demonstrate clearly that structural changes in the materials occur during processing, heat-treatment and, in some cases, catalytic testing, these techniques do not have the spatial resolution (SEM) or limit of detection (powder XRD) necessary to unambiguously determine the nanostructure of the materials, much less elucidate catalysis mechanism.

⁻⁻ indicates light-off not achieved

REFERENCES

- Maleki H, Hüsing N (2018) Current status, opportunities and challenges in catalytic and photocatalytic applications of aerogels: Environmental protection aspects. Appl Catal B Environ 221:530–555. https://doi.org/10.1016/J.APCATB.2017.08.012
- 2. Pajonk GM (1999) Some catalytic applications of aerogels for environmental purposes. Catal Today 52:3–13. https://doi.org/10.1016/S0920-5861(99)00057-7
- 3. Ingale SV, Wagh PB, Tripathi AK, Dudwadkar AS, et al. (2011). Photo catalytic oxidation of TNT using TiO 2-SiO 2 nano-composite aerogel catalyst prepared using sol–gel process. Journal of sol-gel science and technology, 58(3), 682-688.
- 4. Pierre AC, Pajonk GM (2002) Chemistry of Aerogels and Their Applications. Chem Rev 11:4243–4266. https://doi.org/10.1021/CR0101306
- 5. Heywood JB (2018) Internal combustion engine fundamentals. McGraw-Hill Education, New York.
- Bossi T, Gediga J (2017) The environmental profile of platinum group metals interpretation of the
 results of a cradle-to-gate life cycle assessment of the production of pgms and the benefits of their
 use in a selected application. Johnson Matthey Technol Rev 61:111–121.
 https://doi.org/10.1595/205651317X694713
- 7. Heck RM, Farrauto RJ, Gulati ST (2009) Catalytic air pollution control: commercial technology, John Wiley & Sons, New Jersey.
- 8. Keysar S, Shter GE, de Hazan Y, et al. (1997) Heat Treatment of Alumina Aerogels. Chem Mater 9:2464–2467. https://doi.org/10.1021/CM970208S
- Bouck RM, Anderson AM, Prasad C, et al. (2016) Cobalt-alumina sol gels: Effects of heat treatment on structure and catalytic ability. J Non Cryst Solids 453. https://doi.org/10.1016/j.jnoncrysol.2016.09.013
- 10. Juhl SJ, Dunn NJH, Carroll MK, et al. (2015) Epoxide-assisted alumina aerogels by rapid supercritical extraction. J Non Cryst Solids 426. https://doi.org/10.1016/j.jnoncrysol.2015.06.030
- 11. Gauthier BM, Bakrania SD, Anderson AM, Carroll MK (2004) A fast supercritical extraction technique for aerogel fabrication. J Non Cryst Solids 350. https://doi.org/10.1016/j.jnoncrysol.2004.06.044
- 12. Carroll MK, Anderson AM, Gorka CA (2014) Preparing silica aerogel monoliths via a rapid supercritical extraction method. J Vis Exp. https://doi.org/10.3791/51421

- 13. Anderson AM, Bruno BA, Donlon EA, et al. (2018) Fabrication and testing of catalytic aerogels prepared via rapid supercritical extraction. J Vis Exp. https://doi.org/10.3791/57075
- 14. Bono MS, Anderson AM, and Carroll MK (2010). Alumina aerogels prepared via rapid supercritical extraction. Journal of sol-gel science and technology, 53(2), 216-226.
- 15. Tobin ZM, Posada LF, Bechu AM, et al. (2017) Preparation and characterization of copper-containing alumina and silica aerogels for catalytic applications. J Sol-Gel Sci Technol 84. https://doi.org/10.1007/s10971-017-4425-9
- 16. Anderson AM, Donlon EA, Forti AA, et al. (2017) Synthesis and characterization of coppernanoparticle-containing silica aerogel prepared via rapid supercritical extraction for applications in three-way catalysis. In: MRS Advances
- Posada LF, Carroll MK, Anderson AM, Bruno BA (2019) Inclusion of Ceria in Alumina- and Silica-Based Aerogels for Catalytic Applications. J Supercrit Fluids 152. https://doi.org/10.1016/j.supflu.2019.05.004
- 18. Anderson AM, Bruno BA, Dilone F, et al. (2020) Effect of Copper Loading in Copper-Alumina Aerogels on Three-Way Catalytic Performance. Emiss Control Sci Technol 6. https://doi.org/10.1007/s40825-020-00165-z
- 19. Nosrati RH, Berardi U (2018) Hygrothermal characteristics of aerogel-enhanced insulating materials under different humidity and temperature conditions. Energy Build 158:698–711. https://doi.org/10.1016/J.ENBUILD.2017.09.079
- 20. Armor JN, Carlson EJ (1985) A novel procedure for "pelletizing" aerogels. Appl Catal 19:327–337. https://doi.org/10.1016/S0166-9834(00)81755-8
- 21. Domínguez M, Taboada E, Molins E, Llorca J (2008) Co–SiO2 aerogel-coated catalytic walls for the generation of hydrogen. Catal Today 138:193–197. https://doi.org/10.1016/J.CATTOD.2008.05.027
- 22. Domínguez M, Taboada E, Molins E, Llorca J (2012) Co-Fe-Si Aerogel Catalytic Honeycombs for Low Temperature Ethanol Steam Reforming. Catal 2012, Vol 2, Pages 386-399 2:386–399. https://doi.org/10.3390/CATAL2030386
- 23. Lee KJ, Choe YJ, Kim YH, et al. (2018) Fabrication of silica aerogel composite blankets from an aqueous silica aerogel slurry. Ceram Int 44:2204–2208. https://doi.org/10.1016/J.CERAMINT.2017.10.176

- 24. Landau MV, Shter GE, Titelman L, et al. (2006) Alumina Foam Coated with Nanostructured Chromia Aerogel: Efficient Catalytic Material for Complete Combustion of Chlorinated VOC. Ind Eng Chem Res 45:7462–7469. https://doi.org/10.1021/IE0606744
- 25. Reichenauer G, Scherer GW (2001) Nitrogen sorption in aerogels. J Non Cryst Solids 285:167–174. https://doi.org/10.1016/S0022-3093(01)00449-5
- 26. Bruno BA, Anderson AM, Carroll M, et al. (2016) Benchtop Scale Testing of Aerogel Catalysts: Preliminary Results. SAE Tech Pap. https://doi.org/10.4271/2016-01-0920
- 27. Rappé KG, DiMaggio C, Pihl JA, et al. (2019) Aftertreatment Protocols for Catalyst Characterization and Performance Evaluation: Low-Temperature Oxidation, Storage, Three-Way, and NH 3 -SCR Catalyst Test Protocols. Emiss Control Sci Technol 2019 52 5:183–214. https://doi.org/10.1007/S40825-019-00120-7
- 28. Schlatter JC (1978) Water-Gas Shift and Steam Reforming Reactions Over a Rhodium Three-Way Catalyst. SAE Tech Pap. https://doi.org/10.4271/780199
- 29. Sisk CN, Hope-Weeks LJ (2008) Copper (II) aerogels via 1, 2-epoxide gelation. J Mater Chem 18:2607–2610. https://doi.org/10.1039/B802174K
- 30. Gonçalves R V., Wojcieszak R, Wender H, et al. (2015) Easy Access to Metallic Copper Nanoparticles with High Activity and Stability for CO Oxidation. ACS Appl Mater Interfaces 7:7987–7994. https://doi.org/10.1021/ACSAMI.5B00129
- 31. Barbier J, Duprez D (1994) Steam effects in three-way catalysis. Appl Catal B Environ 4:105–140. https://doi.org/10.1016/0926-3373(94)80046-4

Statements and Declarations

Funding

This work was supported by National Science Foundation (NSF) Grants No. IIP-1918217, IIP-1823899, DMR-1828144 and CBET-1228851.

Competing Interests

The authors have no relevant financial or non-financial interests to disclose.

Author Contributions

Ann M. Anderson: Conceptualization, Methodology, Investigation, Data Curation, Writing - Original Draft, Writing - Review & Editing, Supervision, Project administration, Funding acquisition Bradford A. Bruno: Conceptualization, Methodology, Investigation, Data Curation, Writing - Original Draft, Writing - Review & Editing, Supervision, Project administration, Funding acquisition Joana Santos: Writing - Review & Editing, Investigation, Data Curation Chris Avanessian: Writing - Review & Editing, Investigation, Data Curation Mary K. Carroll: Conceptualization, Methodology, Investigation, Data Curation, Writing - Original Draft, Writing - Review & Editing, Supervision, Project administration, Funding acquisition